

Unusual Saddle-like Structure of (2-MeOC₆H₄CS)₂S: Theoretical Studies and Comparison with its Oxygen Isologues

Osamu Niyomura,^[a] Yuka Kito,^[a] Shinzi Kato,^{*[b]} Masaru Ishida,^[a] Masahiro Ebihara,^[a] Satoko Hayashi,^[c] and Waro Nakanishi^{*[c]}

Keywords: Acyl thioacyl sulfides; Bis(thioacyl) sulfides; MO calculation; Molecular structure; X-ray diffraction

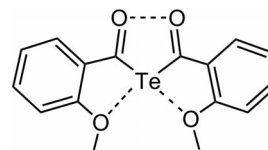
Abstract. Compound (2-MeOC₆H₄CS)₂S (**1**) showed an unusual saddle structure in which the –C(=S)–S–C(=S)– moiety is planar and two benzene rings lie a face-to-face and the distances (3.07 Å) between the central sulfur atom and two 2-methoxy oxygen atoms are within the sum of van der Waals radii of the both atoms. However, the results of MO calculation at the B3LYP/6-311+G(2d,p) level showed no orbital interaction between both atoms. From the results of the calculations at the MP2 level, it was deduced that the crystal packing effect is important for such densely packed crystal, due to its less effective volume. On the other hand, the *para*-methoxy derivative (4-MeOC₆H₄CS)₂S (**2**) in which the two methoxy oxygen atoms are not able to contact

with the central sulfur atom shows an L-shaped structure in which the –C(=S)–S–C(=S)– moiety is not planar. The –C(=O)–S–C(=S)– moiety in compound (2-MeOC₆H₄CO)(2-MeOC₆H₄CS)S (**3b**) shows an L-shaped structure, though the two methoxy oxygen atoms are in intramolecular contact with the central sulfur atom. The deep blue to green colors of compounds **1** and **2** and the deep violet color of compound **3b** are due to transitions of the lone-pair electrons in the HOMO (ψ_{87}) of the thiocarbonyl sulfur atom to the LUMO (ψ_{89}) and of those in the HOMO (ψ_{83}) of the thiocarbonyl sulfur atom to the LUMO (ψ_{85}), respectively.

Introduction

In a previous paper, we stated that bis(2-methoxybenzoyl) telluride, which is a tellurium isologue of acid anhydrides, is nearly planar with intramolecular interactions between the two methoxy oxygen atoms and the central tellurium and between the two carbonyl oxygen atoms^[1] (Scheme 1). Although we reported the syntheses of a series of acyl thioacyl^[2] and bis(thioacyl) sulfides,^[3] X-ray molecular structure analyses have not yet been performed. To the best of our knowledge, only the structures of cyclic acyl thioacyl and bis(thioacyl) sulfides^[4,5] and an acyclic sulfide (4-MeC₆H₄CS)₂S^[6] have been described in the literature. We describe here an unusual

saddle structure of bis(2-methoxybenzenecarbothioyl) sulfide and theoretical studies for a series of the corresponding acyl thioacyl and diacyl sulfides and acid anhydride RC(E²)E¹C(E³)R (R = 2-MeOC₆H₄, 4-MeOC₆H₄; E², E¹, E³ = O, S).



Scheme 1. (2-MeOC₆H₄CO)₂Te.

Results and Discussion

Preparation of Acyl Thioacyl Sulfides (3)

For the preparation of compounds of type **3**, the previous method^[2] using acyl chloride with sodium carbodithioates is disadvantageous with regard to purification of the products due to the difficulty of removing unreacted acyl chlorides and by-product NaCl. We found that the use of potassium carbodithioates instead of the sodium salts leads to the complete reaction of acyl chlorides, a shorter reaction time and easy removal of by-product KCl. (Scheme 2)

Molecular Structures

The molecular structure of bis(2-methoxybenzenecarbothioyl) sulfide (**1**) is shown in Figure 1 along with that of bis(4-methoxybenzenecarbothioyl) sulfide (**2**)^[2] for compari-

* Prof. S. Kato
Fax: +81-52-222-2442
E-mail: kshinzi@nifty.com

* Prof. W. Nakanishi
E-Mail: nakanisi@sys.wakayama-u.ac.jp

[a] Department of Chemistry
Faculty of Engineering
Gifu University

Gifu 501-1193, Japan

Present address: Maruno-uchi 2-14-32,

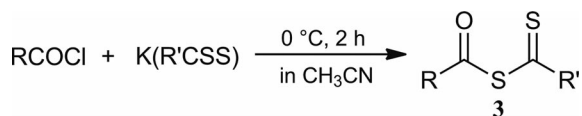
Lions-City Maruno-uchi 1105
Naka-ku, Nagoya 460-0002, Japan

[b] Department of Applied Chemistry
College of Engineering
Chubu University

Kasugai 487-8501, Japan

[c] Department of Material Science
Faculty of Systems Engineering and Chemistry
Wakayama University
Wakayama, 650-8510, Japan

Supporting information for this article is available on the WWW under <http://dx.doi.org/10.1002/zaac.201200357> or from the author.



No.	R	R'	Yield ^{a)} / %
3a	4-MeC ₆ H ₄	4-MeC ₆ H ₄	63
3b	2-MeOC ₆ H ₄	2-MeOC ₆ H ₄	81
3c		4-MeC ₆ H ₄	90
3d	4-MeOC ₆ H ₄	4-MeC ₆ H ₄	62
3e		2-MeOC ₆ H ₄	75
3f		4-MeOC ₆ H ₄	76
3g	4-ClC ₆ H ₄	4-MeC ₆ H ₄	55
3h		4-MeOC ₆ H ₄	62

a) Isolated yield.

Scheme 2.

son. Their crystal data and data-collection parameters as well as selected bond lengths and angles are summarized in Table 1 and Table 2, respectively.

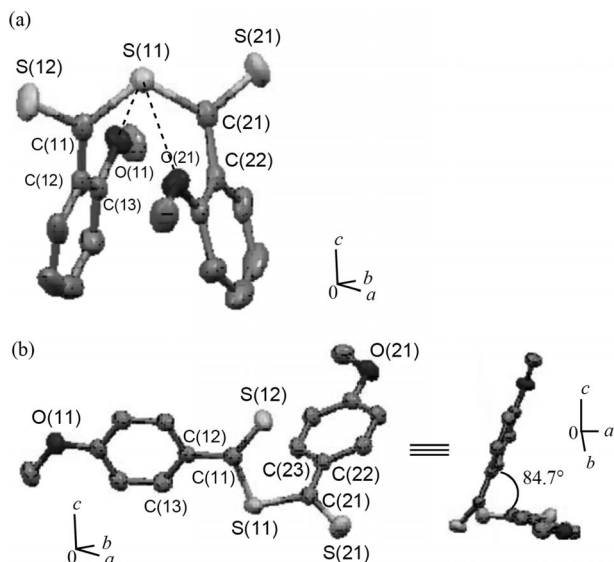


Figure 1. Molecular structures of (2-MeOC₆H₄CS)₂S (**1**) (a) and (2-MeOC₆H₄CS)₂S (**2**) (b). All hydrogen atoms have been omitted for clarity. The thermal ellipsoid plots represent 50% probability.

Compound **1** has a C₂ symmetry axis through the central sulfur atom S(11), where the [–C(11)=S(12)–S(11)–C(21)=S(21)–] moiety is planar and the two methoxy groups are situated opposite each other across the C(11)–S(11)–C(21) plane (Figure 1 (a)). The C(11)–S(11)–C(21) and O(11)···S(11)···O(21) planes cross each other at nearly a right angle on the central sulfur atom S(11). The O(11)···S(11) and O(21)···S(11) distances are both almost 3.07 Å, which is significantly shorter than the sum of the van der Waals radii of the two atoms (3.32 Å) (Figure 2, (a)). Moreover, the two benzene rings with a dihedral angle of *approx.* 27° are situated very close together to give a nearest plane-to-plane distance of 3.18 Å (C(13)···C(22)), which is comparable to the sum of the van der Waals radii of both carbon atoms (3.42 Å) (Figure 2,

(b)), which suggests that there may be weak intramolecular π–π interaction between the carbon atoms. Presumably, a twisted conformation associated with the benzene ring and dithiocarbonyl group may allow for this face-to-face approach of the benzene rings. To the best of our knowledge, such an unusual saddle-like structure in which two benzene rings show a face-to-face approach is the first example among carbochalcogenoic anhydrides [RC(E')–E–C(E')–R, E = O, S, Se, Te; E' = O, S].

In the *para*-methoxy derivative **2**, which does not show any intramolecular interaction between the methoxy oxygen and the thiocarbonyl or central sulfur atoms, the interplanar angle S(12)–C(11)···C(21)–S(21) is 84.7(2)°, which reflects an L-shaped structure (Figure 1 (b), right). The S(12)–C(11)–C(12)–C(13) and S(11)–C(21)–C(22)–C(23) torsion angles are 14.7(3)° and –18.9(3)°, respectively, which indicates that there is a small twist between the benzene ring and dithiocarbonyl groups.

The X-ray molecular structure of compound **3b**, in which one of the two thiocarbonyl sulfur atoms of **1** is replaced by an oxygen atom, is shown in Figure 3 along with those of bis(2-methoxybenzoyl) sulfides (**4**)^[1] and 2-methoxybenzoic anhydride (**5**)^[1,7] for comparison.

In compound **3b**, the two benzene-ring planes are considerably twisted from the planes of the associated –C(O)S– or –C(S)S– groups (C(21)–S(11)–C(11)–C(12) = 32.8(2)°; S(11)–C(11)–C(12)–C(13) = 53.3(3)°, respectively). The O(11)···S(11) and O(12)···S(11) distances are 2.663(2) Å and 3.117(2) Å, respectively, which are shorter than the sum of the van der Waals radii of both atoms (3.32 Å), though the distances are significantly different. Such interaction is considered to reflect an intermediate structure between compound **1**, in which both *ortho*-methoxy oxygen atoms are in intramolecularly contact with the central sulfur atom and compound **4**, in which neither of the *ortho*-methoxy oxygen atoms are in intramolecular contact with the central atom. The O(12)···S(11)–C(21) linkage in compound **3b** is nearly linear (175.8°), suggesting that the strength of the O(12)···S(11) interactions may be enhanced. Moreover, the S(11)–C(11)/S(11)–C(21) distances are apparently different, 1.830(2) Å and 1.758(4) Å, respectively (see below: *ab initio* calculations).

Compound **4** has a –C(O)SC(O)– moiety in which the two C=O groups point in the same direction. The benzene ring planes are appreciably twisted from the plane of the associated –C(O)S– group [O(11)–C(11)–C(12)–C(13)/O(21)–C(21)–C(22)–C(23) = 22.1(1)°/–56.5(2)°], respectively. The O(11)–C(11)···C(21)–O(21) interplanar angle is 30.6°. One of the two *ortho*-methoxy oxygen atoms (O(12)) is in intramolecular contacts with the central sulfur atom S(11), while the other (O(22)) is in contact with the carbonyl oxygen atom O(21). The O(12)···S(11) and O(22)···O(21) distances are 2.719 Å and 2.761 Å, respectively, which are significantly shorter than the sum of the van der Waals radii of both atoms (O···S = 3.32 Å and O···O = 3.04 Å, respectively^[1,7]). The O(21)···O(11) distance (2.761 Å) also suggests weak non-bonding interaction.^[1] The linearity of both the O(12)···S(11)–C(21) (173.5°) and O(11)···O(21)···O(22) linkages (143.5°)

Table 1. Crystal data and data collection of (2-MeOC₆H₄CS)₂S (**1**), (4-MeOC₆H₄CS)₂S (**2**), and (2-MeOC₆H₄CO)(2-MeOC₆H₄CS)S (**3b**).

	compound 1 ^{a)}	compound 2 ^{b)}	compound 3e ^{c)}
empirical formula	C ₁₆ H ₁₄ O ₂ S ₃	C ₁₆ H ₁₄ O ₂ S ₃	C ₁₆ H ₁₄ O ₃ S ₂
formula weight	334.45	334.45	318.39
color	darkgreen, prismatic	darkgreen, prismatic	dark blue, prismatic
crystal system	tetragonal	monoclinic	monoclinic
unit-cell dimensions	<i>a</i> = 7.737(2) Å <i>b</i> = 7.737(2) Å <i>c</i> = 13.290(4) Å	<i>a</i> = 7.359(5) Å <i>b</i> = 14.512(7) Å <i>c</i> = 14.734(4) Å	<i>a</i> = 14.022(3) Å <i>b</i> = 7.544(4) Å <i>c</i> = 14.041(3) Å
β /°	795.6(4)	98.74	95.58(2)
volume of unit cell /Å ³	1414.4(3)	1555.2(5)	1478.3(8)
space group	<i>P</i> 42	<i>P</i> 21/ <i>c</i>	<i>P</i> 21/ <i>c</i>
<i>Z</i> value	2	4	4
<i>D</i> _{calc} /g cm ⁻³	1.396	1.428	1.431
crystal size /mm	0.34 x 0.29 x 0.29	0.54 x 0.37 x 0.31	0.34 x 0.17 x 0.14
μ (Mo- <i>K</i> α) /cm ⁻¹	4.66	4.76	3.66
temp /°C	-80.0	-80.0	-80.0
λ _{Mo-<i>K</i>α} /Å	0.71069	0.71069	0.71069
2 θ _{max} /deg	55.0°	55.0°	55.0°
no. of measured reflections	1082	3841	3540
no. of observations (<i>I</i> > 2 σ (<i>I</i>))	950	3572	3405
no. of variables	192	192	192
residuals: <i>R</i> , ^{d)} <i>R</i> _w ^{e)} [<i>I</i> > 2 σ (<i>I</i>)]	0.028, 0.025	0.0335, 0.0791	0.0402, 0.1098
<i>R</i> indices (all data)	0.0401, 0.0798	0.0601, 0.0894	0.0696, 0.1106
goodness of fit on <i>F</i> ²	1.87	1.012	1.014

a) CCDC-720120. b) CCDC-720120. c) CCDC-720122. d) $R = \sum(|F_o| - |F_c|) / \sum |F_o|$.

e) $R_w = [\sum (|F_o| - |F_c|)^2 / \sum w |F_o|^2]^{1/2}$, $w = [\sigma^2(F_o) + p^2(F_o)^2/4]^{-1}$.

Table 2. Selected bond lengths /Å, angles /° and torsion angles /° of (2-MeOC₆H₄CS)₂S (**1**), (4-MeOC₆H₄CS)₂S (**2**), and (2-MeOC₆H₄CO)(2-MeOC₆H₄CS)S (**3b**).

Compound (1)		Bond lengths		Angles	
S(12)–C(11)	1.638(1)	O(11)···S(11)	3.069(2)	C(11)–S(11)–C(21)	112.2(1)
S(21)–C(21)	1.638(1)	O(21)···S(11)	3.069(2)	S(12)–C(11)–S(11)	113.2(2)
S(11)–C(11)	1.752(2)	S(12)···S(11)	2.832(2)	S(21)–C(21)–S(11)	113.3(1)
S(11)–O(21)	1.752(2)	S(21)···S(11)	2.832(2)	O(11)–S(11)–O(21)	108.0(2)
Torsion angles					
S(21)–C(21)–S(11)–C(11)	162.2(2)	C(11)–S(11)–C(21)–C(23)	20.2(1)	S(11)···S(11)···S(21)–C(21)	14.7(2)
S(12)–C(11)–S(11)–C(21)	162.3(3)	S(21)–C(11)–C(12)–C(13)	45.5(1)	S(11)–C(11)···C(21)–S(21)	57.9(1)
Compound (2)		Bond lengths		Angles	
S(12)–C(11)	1.633(2)	C(21)–S(11)	1.791(2)	C(11)–S(11)–C(21)	103.4(1)
S(21)–C(21)	1.629(2)	S(11)···S(12)	2.909(2)	S(11)–C(11)–S(12)	121.4(1)
C(11)–S(11)	1.772(2)	S(11)···S(21)	2.969(1)	S(21)–C(21)–S(11)	116.3(2)
Torsion angles					
S(12)–C(11)–S(11)–C(21)	124.1(2)	S(11)–C(11)–C(12)–C(13)	-18.9(2)	S(12)–C(11)···C(21)–S(21)	84.7(1)
S(21)–C(21)–S(11)–C(11)	-17.2(2)	S(11)–C(21)–C(22)–C(23)	14.7(2)	C(12)–C(11)–S(11)–C(21)	61.6(2)
Compound (3b)		Bond lengths		Angles	
S(21)–C(21)	1.625(3)	O(11)···S(11)	3.069(2)	S(11)–C(11)–C(12)	104.3(1)
O(11)–C(11)	1.209(3)	O(21)···S(11)	3.069(2)	S(11)–C(21)–C(22)	121.6(2)
S(11)–C(11)	1.830(2)	O(11)···O(12)	3.208(2)	O(11)–S(11)–C(11)	115.0(1)
S(11)–C(21)	1.758(2)	O(21)···S(11)–C(11)		O(11)–S(11)–C(11)	123.3(2)
Torsion angles					
O(11)–C(11)–S(11)–C(21)	32.5(4)	O(11)–C(11)–C(12)–C(12)	34.3(2)	C(21)–S(11)–C(11)–C(12)	32.8(2)
S(21)–C(21)–S(11)–C(11)	170.4(6)	S(21)–C(21)–C(22)–C(27)	22.6(3)	S(11)–C(11)–C(12)–C(13)	53.3(3)

suggests that the orbital interactions between O(12)···S(11) and between O(21)···O(22) may be enhanced.

On the other hand, the corresponding acid anhydride (2-MeOC₆H₄CO)₂O (**5**) assumes an L-shaped structure in contrast to compound **4** (O(13)···O(11)···C(22) angle is 76.4(2)°) (Figure 3 (c), right). One of the benzene ring planes is considerably twisted from the plane of the associated –COO– group (torsion

angle: O(21)–C(21)–C(22)–C(23) = -142.3(1)°, while the other and the plane of the other associated –C(O)O– group are almost coplanar (torsion angle O(11)–C(11)–C(12)–C(13) = 6.5(2)°). Both the O(11)···O(13) and O(21)···O(22) distances are short at 2.691(2) Å and 2.651(3) Å, respectively, and the O(13)···C(11) and O(22)···C(21) distances are 2.842(2) Å and 2.780(2) Å, respectively. These are significantly shorter than

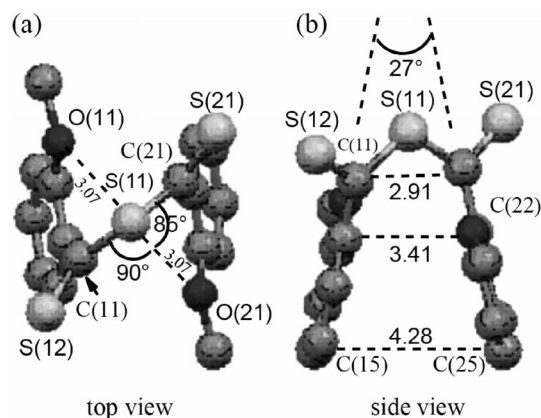


Figure 2. Top (a) and side views (b) of compound **1** (distances in Å).

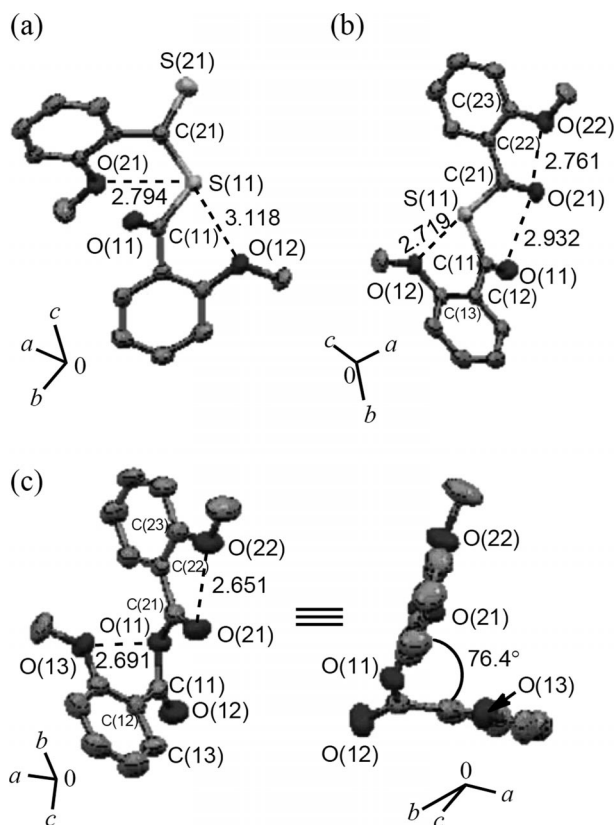
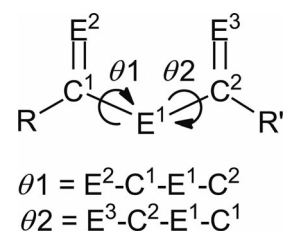


Figure 3. Molecular structures of (a) (2-MeOC₆H₄CO)(2-MeOC₆H₄CS)S (**3b**), (b) (2-MeOC₆H₄CO)₂S (**4**), and (c) (2-MeOC₆H₄CO)₂O (**5**). All hydrogen atoms have been omitted for clarity. Black dotted lines show intramolecular short contacts. Distances are given in Å. The thermal ellipsoid plots represent 50% probability.

the sum of the van der Waals radii of both atoms (3.04 Å), which suggests intramolecular interactions between the methoxy oxygen atom and the carbonyl group. Thus, one of the two *ortho*-methoxy oxygen atoms is in contact with the central oxygen atom, while the O(22) is in contact with the carbonyl oxygen O(21) (Figure 3 (c), left).^[7]

Regarding the conformers of acid anhydrides, the torsion angles θ_1 and θ_2 in the $-C(E^2)E^1C(E^3)-$ moiety ($E^1, E^2, E^3 = O, S$) were defined (Scheme 3), and their conformation were

determined according to the values of θ_1 and θ_2 as synperiplanar (sp), synclinal (sc), anticlinal (ac), or antiperiplanar (ap) [8]. Table 3 shows the conformations of compounds **1**, **2**, **3b**, **4**, and **5** along with the torsion angles (θ_1 and θ_2). The angles θ_1 and θ_2 vary remarkably ($9^\circ < \theta_1/\theta_2 < 172^\circ$) according to the number of sulfur atoms replaced by a $-C(E^2)E^1C(E^3)-$ moiety, so that compounds **1**, **2**, **3b**, **4**, and **5** adopt various conformations (ap/ap, ac/sp, sc/ap, sp/sp and sp/ac, respectively). For compounds **1**, **3b**, **4**, and **5**, which have *o*-methoxy groups, the ap conformation is preferable for the carbothioate ($-\text{COS}-$) or carbodithioate groups ($-\text{CSS}-$), while the sp conformation is more advantageous than ap for the carbothioate group ($-\text{COS}-$). Moreover, the conformations of bis(thioaroyl) sulfides (**1** and **2**) are influenced by the position of the substituents on the benzene ring, i.e., an *ortho*-substituent leads to an [ap/ap] conformation, whereas a *para*-substituent leads to an [sp/ac] conformation.



Scheme 3.

Intermolecular Short Contacts and Molecular Arrangement

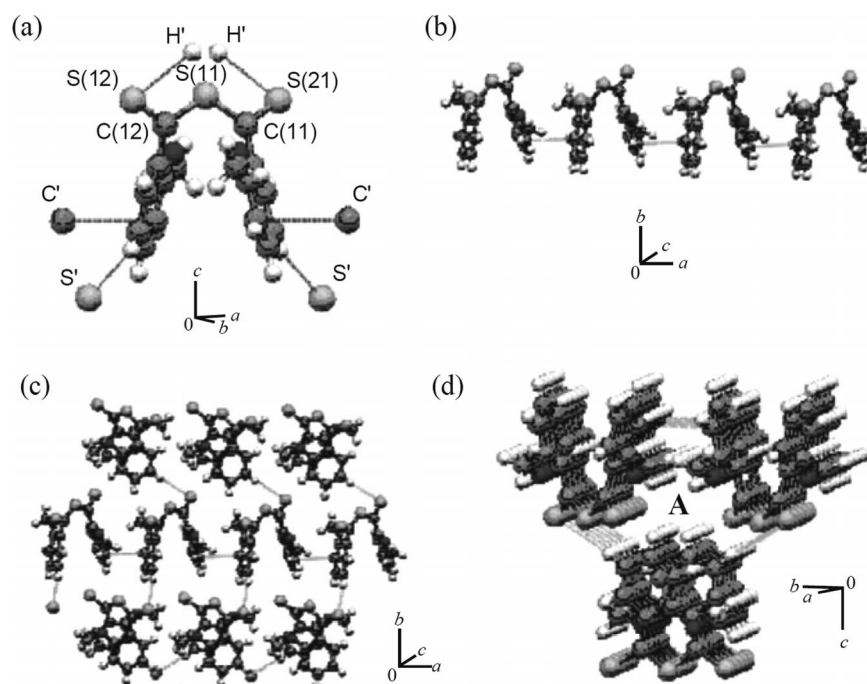
The arrangements of compounds **1** and **2**, **3b**, **4**, and **5** formed by $\text{S}\cdots\text{H}$ and $\text{O}\cdots\text{H}$ hydrogen bonding interactions and $\text{S}\cdots\text{S}$, $\text{S}\cdots\text{C}$, $\text{O}\cdots\text{C}$, $\text{C}\cdots\text{C}$ and $\text{C}\cdots\text{H}$ short contacts are shown in Figure 4 and in the Supporting Information Figure S1, respectively.

For compound **1**, intermolecular $\text{S}\cdots\text{H}$ hydrogen bonding and $\text{C}-\text{C}/\pi$ interactions are observed between the thiocarbonyl sulfur and benzene-ring hydrogen atoms, and between the benzene ring-carbon atoms, respectively (Figure 4, (a)). The molecules are arranged linearly by the CC/π interactions between the benzene-ring carbon atoms (Figure 4, (b)). The linearly arranged molecules have intermolecular contacts between the thiocarbonyl sulfur and benzene-ring hydrogen atoms, to give a molecular sheet as shown in Figure 4, (c). Moreover, these sheets are stacked vertically with respect to each other to form 3D networks by intermolecular contacts, in which columns such as **A** (9.7×7.6 Å) are formed (Figure 4, (d)).

For the *para*-methoxy derivative **2**, intermolecular $\text{S}\cdots\text{H}$ and $\text{O}\cdots\text{H}$ hydrogen bonds between the thiocarbonyl sulfur and methoxy-methyl hydrogen atoms and between the methoxy oxygen and methoxy-methyl hydrogen atoms, respectively, and weak $\text{S}\cdots\text{S}$, $\text{S}\cdots\text{C}$ and $\text{O}\cdots\text{C}$ short contacts between the thiocarbonyl sulfur atoms, between the thiocarbonyl sulfur and benzene-ring carbon atoms and between the methoxy oxygen and methoxy-methyl carbon atoms, respectively, are observed along with weak CH/π interactions both between the methoxy-

Table 3. Conformations and torsion angles of compounds 1–5.

Compounds	(2-MeOC ₆ H ₄ CS) ₂ S	(4-MeOC ₆ H ₄ CS) ₂ S	2-MeOC ₆ H ₄ CO- 2-MeOC ₆ H ₄ CS ⁻ S	(2-MeOC ₆ H ₄ CO) ₂ S	(2-MeOC ₆ H ₄ CO) ₂ O
	1	2	3b	4	5
Conformation	ap/ap	ac/sp	sp/ap	sp/sp	sp/ac
Torsion angle /° (θ1/θ2)	162.2(2)/162.2(2)	17.1(1)/124.2(1)	-32.5(2)/170.4(1)	-26.8(2)/-9.4(2)	-17.2(2)/124.2(1)

**Figure 4.** Intermolecular short contacts and molecular arrangement of (2-MeOC₆H₄CS)₂S (**1**). Dotted lines in (b)–(d) show intermolecular short contacts. (a) The atoms denoted with a prime show neighboring molecules. (b) The one-dimensional linear chain formed by short contacts between benzene-ring carbon atoms. (c) Two-dimensional sheet formed by the S⋯H hydrogen bonding between the thiocarbonyl sulfur and benzene-ring hydrogen atoms and the C⋯C short contacts between benzene-ring carbon atoms. (d) 3D networks formed by stacking of these sheets.

methyl hydrogen and the benzene-ring carbon atoms and between the benzene-ring hydrogen and carbon atoms^[9] (Figure S1 (a)).

The molecules of *para*-methoxy derivative **2** are arranged linearly by both hydrogen bonding between the methoxy oxygen and methoxy-methyl hydrogen atoms and weak O⋯C short contacts between the methoxy oxygen and the methoxy-methyl carbon atoms (Figure 5, (a)). The linearly arranged molecules have intermolecular contacts between the methoxy oxygen and methoxy-methyl hydrogen atoms and weak O⋯C short contacts between the methoxy oxygen and methoxy-methyl carbon atoms, to form a ladder and sheet as shown in (Figure 5, (b)). Moreover, these sheets are stacked vertically with respect to each other to form 3D networks by intermolecular contacts, in

which rectangular columns such as **A** (10.2 × 4.4 Å) are formed (Figure 5, (c)).

In the case of (acyl)(thioacyl) sulfide **3b**, intermolecular O⋯H hydrogen bonds between the carbonyl oxygen and both methoxy-methyl and benzene-ring hydrogen atoms and between the methoxy oxygen and methoxy-methyl hydrogen atoms, respectively, and weak S⋯C short contacts between the thiocarbonyl sulfur and benzene-ring carbon atoms are observed along with weak CH/π interactions between the methoxy-methyl hydrogen and benzene-ring carbon atoms^[9] (Figure S1 (b)). The molecules are arranged linearly by hydrogen bonds between the carbonyl oxygen and benzene-ring hydrogen atoms (Figure 6, (a)). Short intermolecular contacts between the methoxy-methyl hydrogen and the benzene-ring car-

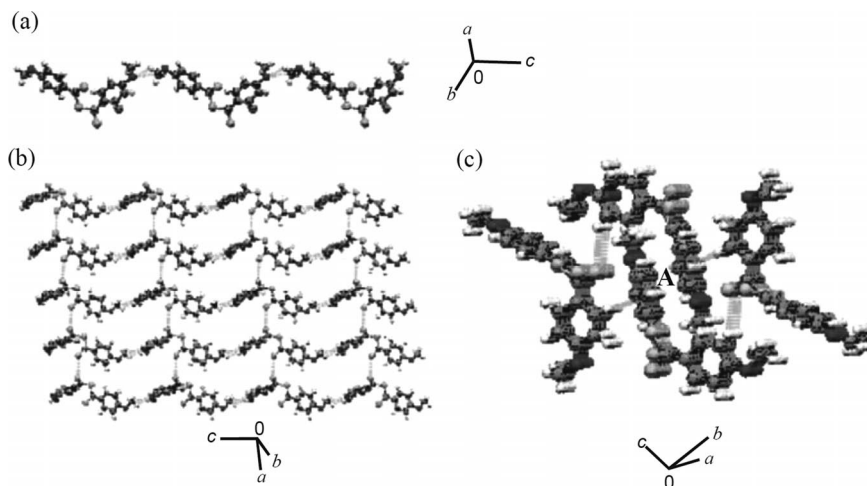


Figure 5. Molecular arrangement of (4-MeOC₆H₄CS)₂S (**2**). Dotted lines show intermolecular short contacts. a) One-dimensional linear chain formed by short contacts between methoxy oxygen and hydrogen and/or carbon atoms. b) Two-dimensional sheet formed by the S...S short contacts between the thiocarbonyl sulfur atoms. c) 3D Networks formed by stacking of these sheets.

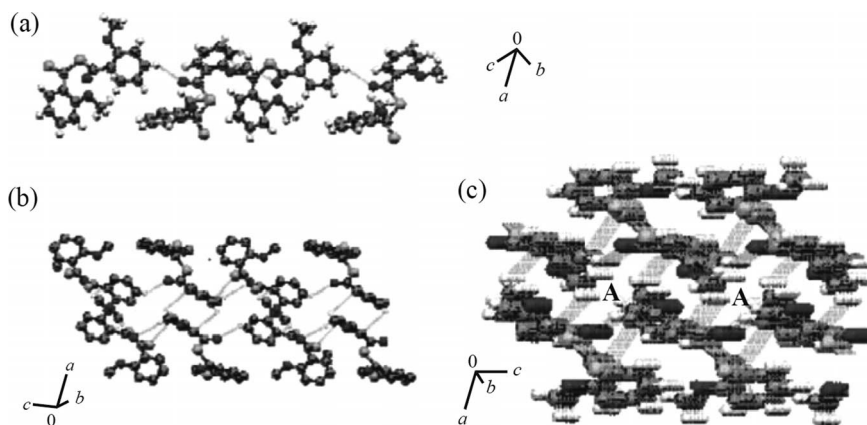


Figure 6. Molecular arrangement of (2-MeOC₆H₄CO)(2-MeOC₆H₄CS)S (**3b**). Dotted lines show intermolecular short contacts. (a) One-dimensional linear chain formed by hydrogen bonding between benzene ring hydrogen and carbonyl oxygen atoms. (b) Two-dimensional sheet formed by the above hydrogen bonding and the S...H hydrogen bonding between the thiocarbonyl sulfur and benzene-ring hydrogen atoms. (c) 3D Networks formed by stacking of these sheets.

bon atoms form a planar sheet (Figure 6, (b)). Moreover, these sheets are stacked vertically with respect to each other to form 3D networks by intermolecular contacts, in which rectangular channels such as **A** ($7.8 \times 4.5 \text{ \AA}$) are formed (Figure 6, (c)).

For diacyl sulfide (**4**), O...H hydrogen bonds between the carbonyl oxygen and methoxy-methyl and benzene-ring hydrogen atoms are observed along with weak CH/ π interactions between the methoxy-methyl hydrogen and the benzene-ring carbon atoms^[9] (Figure S1 (c)). The molecules are arranged linearly by hydrogen bonding between the carbonyl oxygen and benzene-ring hydrogen atoms (Figure 7, (a)). The linearly arranged molecules have intermolecular O...H hydrogen bonds between the carbonyl oxygen and methoxy-methyl hydrogen atoms to form a planar sheet (Figure 7, (b)). Moreover, these sheets are stacked vertically with respect to each other to form 3D networks by intermolecular contacts, in which rectangular channels such as **A** ($10.5 \times 4.2 \text{ \AA}$) are formed (Figure 7, (c)).

On the other hand, for the acid anhydride **5**, intermolecular O...H hydrogen bonds between the carbonyl oxygen and both methoxy-methyl and benzene-ring hydrogen atoms are observed along with weak CH/ π interactions between the benzene-ring carbon and the methoxy-methyl hydrogen atoms^[9] (Figure S1 (d)). The molecules are arranged linearly by hydrogen bonds between the carbonyl oxygen and methoxy-methyl hydrogen atoms (Figure 8, (a)). These molecular chains form intermolecular O...H hydrogen bonds between the carbonyl oxygen and methoxy-methyl hydrogen atoms to give a ladder and sheet (Figure 8, (b)). Moreover, through stacking, these sheets form 3D networks, in which columns such as **A** ($6.5 \times 3.3 \text{ \AA}$) are formed (Figure 8, (c)).

Ab initio Calculations

To elucidate the nature of the nonbonding interactions for compounds (2-MeOC₆H₄CS)₂S (**1**), (4-MeOC₆H₄CS)₂S (**2**),

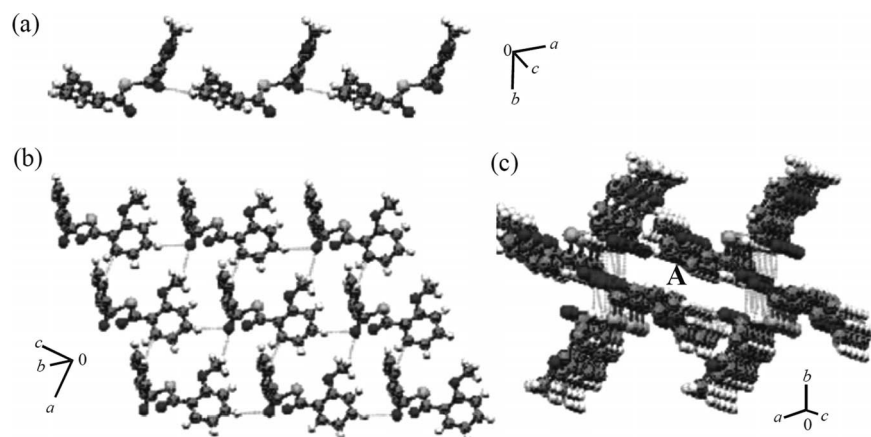


Figure 7. Molecular arrangement of (2-MeOC₆H₄CO)₂S (**4**). Dotted lines show intermolecular short contacts. (a) One-dimensional linear chain formed by C=O...H hydrogen bond between benzene ring hydrogen carbonyl oxygen atoms. (b) Two-dimensional sheet formed by the O...H hydrogen bonds between the carbonyl oxygen and methoxy-methyl and benzene-ring hydrogen atoms. (c) 3D Networks formed by stacking of these sheets.

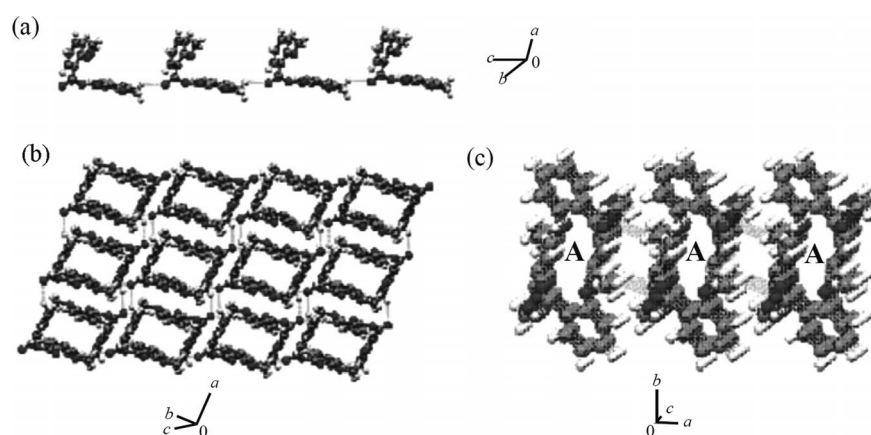


Figure 8. Molecular arrangement of (2-MeOC₆H₄CO)₂O (**5**). Dotted lines show intermolecular short contacts. (a) One-dimensional linear chain formed by C=O...H₃C hydrogen bond between carbonyl oxygen and methoxy methyl hydrogen atoms. (b) Two-dimensional sheet formed by the O...H hydrogen bonds between the carbonyl oxygen and methoxy methyl and benzene ring hydrogen atoms. (c) 3D Networks formed by stacking of these sheets.

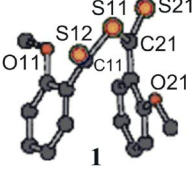
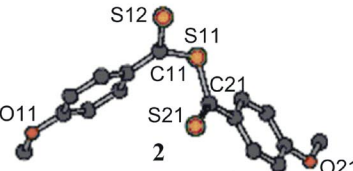
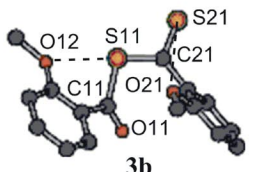
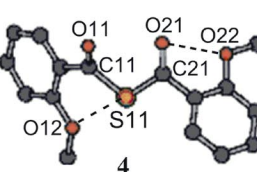
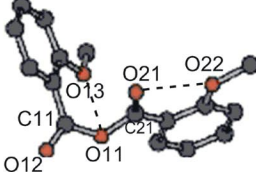
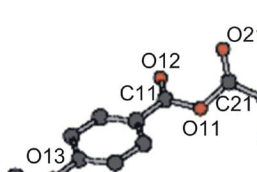
(2-MeOC₆H₄CO)(2-MeOC₆H₄CS)S (**3b**) and (2-MeOC₆H₄CO)₂S (**4**), a natural bond orbital (NBO) analysis was performed at the B3LYP/6-311+G(2d,p) level with Gaussian 03 using X-ray structures.^[10–12] The geometries of compounds (2-MeOC₆H₄CO)₂O (**5**) and (4-MeOC₆H₄CO)₂O (**6**)^[11] were optimized at the B3LYP/6-311+G(2d,p) level with Gaussian 03. The structural optimizations reproduced well the observed structures in crystals, although the calculated structures correspond to those of monomers in vacuo (Supporting Information Table S1). The results of NBO calculations for compounds **1**, **2**, **3b**, **4**, **5**, and **6** are shown in Table 4.

The results for compounds **3b–5** are discussed first, a detailed examination of the results for **1** and **2** follows. NBO calculations for **3b** show three types of appreciable nonbonding orbital interactions, nS(21)→σ*S(11)–C(11), nO(12)→σ*S(11)–C(21) and nO(21)→π*S(21)=C(21), along with nS(11)→π*C(11)=O(11) and nS(11)→π*C(21)=S(21). The delocalization of the lone-pair electrons on the thiocarbonyl and methoxy oxygen atoms to the S(11)–C(11) *anti*-bonding orbital is in

agreement with the experimental observation that the S(11)–C(11) bond length is significantly longer than that of S(11)–C(21). For diacyl sulfide (**4**), there are both nonbonding intramolecular interactions n(O12)→σ*S(11)–C(21) along with delocalization of the lone-pair electrons on the central sulfur atom S(11) to the π* orbitals of thiocarbonyl groups (nS(11)→π*O(11)=C(11) and nS(11)→π*O(21)=C(21)). For acid anhydride (**5**), intramolecular interactions of nO(12)→σ*O(11)–C(21) and nO(22)→π*O(21)–C(21) are present along with the expected localization of the lone-pair electron on the central oxygen atom to the C=O π* orbitals (nO(11)→π*O(12)=C(11) and nO(11)→π*O(21)=C(21)).

On the other hand, orbital interactions spread over the C(11) (=S(12))S(11)C(21) (=S(21)) moiety in **1**, which indicates delocalization of the lone-pair electrons on the thiocarbonyl sulfur atoms to the S–C σ* orbitals (nS(12)→σ*S(11)–C(11) and nS(21)→σ*S(11)–C(21)) along with those on the central sulfur atom S(11) to the π* orbitals of thiocarbonyl groups (nS(11)→π*C(11)=S(12) and nS(11)→π*C(21)=S(21)). How-

Table 4. NBO analyses of (2-MeOC₆H₄CS)₂S (**1**), (4-MeOC₆H₄CS)₂S (**2**), (2-MeOC₆H₄CO)(2-MeOC₆H₄CS)S (**3b**), (2-MeOC₆H₄CO)₂S (**4**), (2-MeOC₆H₄CO)₂O (**5**), and (4-MeOC₆H₄CO)₂O (**6**).

 <p>1</p> <p>ΔE^a [kcal mol⁻¹]</p>			 <p>2</p> <p>ΔE^a [kcal mol⁻¹]</p>		
$n_{S11} \rightarrow \pi^*_{S12=C11}$	$n_{S12} \rightarrow \sigma^*_{S11-C21}$	$n_{S12} \rightarrow \sigma^*_{S11-C11}$	$n_{S11} \rightarrow \pi^*_{S12=C11}$	$n_{S12} \rightarrow \sigma^*_{S11-C21}$	$n_{S12} \rightarrow \sigma^*_{S11-C11}$
24.9	14.9	1.9	42.2	22.9	-
$n_{S11} \rightarrow \pi^*_{S21=C21}$	$n_{S21} \rightarrow \sigma^*_{S11-C11}$	$n_{S21} \rightarrow \sigma^*_{S11-C21}$	$n_{S11} \rightarrow \pi^*_{S21=C21}$	$n_{S21} \rightarrow \sigma^*_{S11-C11}$	$n_{S21} \rightarrow \sigma^*_{S11-C21}$
24.9	14.9	1.9	13.6	18.4	-
 <p>3b</p> <p>ΔE^a [kcal mol⁻¹]</p>			 <p>4</p> <p>ΔE^a [kcal mol⁻¹]</p>		
$n_{S11} \rightarrow \pi^*_{O11=C11}$	$n_{O11} \rightarrow \sigma^*_{S11-C11}$	$n_{O12} \rightarrow \sigma^*_{S11-C21}$	$n_{S11} \rightarrow \pi^*_{O11=C11}$	$n_{O11} \rightarrow \sigma^*_{S11-C11}$	$n_{O12} \rightarrow \sigma^*_{S11-C21}$
25.5	38.2	1.7	27.2	38.2	2.3
$n_{S11} \rightarrow \pi^*_{S21=C21}$	$n_{S21} \rightarrow \sigma^*_{S11-C21}$	$n_{O21} \rightarrow \pi^*_{S21=C21}$	$n_{S11} \rightarrow \pi^*_{O21=C21}$	$n_{O21} \rightarrow \sigma^*_{S11-C21}$	$n_{O22} \rightarrow \pi^*_{O21=C21}$
23.8	16.5	0.9	30.8	41.6	-
 <p>5</p> <p>ΔE^a [kcal mol⁻¹]</p>			 <p>6</p> <p>ΔE^a [kcal mol⁻¹]</p>		
$n_{O11} \rightarrow \pi^*_{O12=C11}$	$n_{O12} \rightarrow \sigma^*_{O11-C21}$	$n_{O13} \rightarrow \sigma^*_{O11-C21}$	$n_{O11} \rightarrow \pi^*_{O12=C11}$	$n_{O12} \rightarrow \sigma^*_{O11-C11}$	$n_{O12} \rightarrow \sigma^*_{O11-C21}$
21.8	41.8	1.4	41.5	36.7	-
$n_{O11} \rightarrow \pi^*_{O21=C21}$	$n_{O21} \rightarrow \sigma^*_{O12=C11}$	$n_{O22} \rightarrow \pi^*_{O21=C21}$	$n_{O11} \rightarrow \pi^*_{O21=C21}$	$n_{O21} \rightarrow \sigma^*_{O11-C21}$	$n_{O21} \rightarrow \sigma^*_{O11-C11}$
41.6	41.5	1.2	41.5	35.6	-

^aAnalyses for the calculation on compounds **1-6** were carried out at B3LYP/6-311+G(2d,p) level of theory for O and S.

ever, there is no orbital interaction between the methoxy oxygen (O(11), O(21)) and central sulfur atoms (S(11)), although the O(11)–S(11) and O(21)–S(11) distances of 3.07 Å are significantly short. In the case of *para*-methoxy derivative **2**, the stabilization effects due to delocalization of the lone-pair electrons on the thiocarbonyl sulfur atoms (S(12) and S(21)) to the *anti*-bonding orbital of the sulfur–carbon bonds (S(11)–C(11) and S(11)–C(21)) are similar at both sites of the central sulfur atom. However, the stabilization energy due to $n_{S(11)} \rightarrow \pi^*_{C(21)=S(21)}$ seems small, presumably due to the substantial twisting of the π -planes of the central sulfur atom and thiocarbonyl group.

The results remind us that some factors other than the intramolecular CT interactions, which can be evaluated by the NBO analysis, would operate to control the crystal structure of **1**,

also apply for compound **2**. What factors operate to control the structures of **1** and **2**? The energy profile of **1** and **2** were investigated, together with the fragment, S(CSPh)₂ (**I**). Structures were optimized with the 6-311+G(2d,p) basis sets at the B3LYP level. The optimized structures were confirmed to be minimal by the frequency analysis. The results are collected in Table 5, together with the relative energies of the conformers. Four conformers are detected in **I**, which are called **A**, **B**, **C**, and **D**.

Conformer **I** (**C**) contains a five-membered cycle of SCSCS atoms. However, it is unlikely to exist as a stable conformer, since the relative energy is too high, relative to **I** (**A**). As a result, conformers **I** (**A**) and **I** (**D**) should be considered as the partial structures of **1** and **2**, respectively, since **I** (**B**) is quite different from **1** and **2**. The results are shown in Figure 9

Table 5. Structures and energies optimized for **1**, **2**, and the fragment, S(CSPh)₂ (**I**).

Compound (Conformer)	$r(^2S^3S)$ /Å	$\angle^1C^1S^2C$ /°	$\phi(^2S^1C^1S^2C)$ /°	$\phi(^1C^1S^2C^1C)$ /°	$\phi(^1S^2C^1C^1C)$ /°	E_{rel} /kJ·mol ⁻¹
B3LYP/6-311+G(2d,p)						
I (A: C ₂)	5.7677	110.68	150.57	-36.42	-31.90	0.0 ^{a)}
I (B: C ₂)	3.4433	110.17	-30.90	153.73	-39.30	1.5
I (C: C ₂)	2.1045	103.80	-17.53	170.70	-0.66	98.3
I (D: C ₁)	4.5718	107.81	-29.22	-177.92	37.38	2.3
			126.05	-60.47	-24.72	
1 (C ₂)	5.7037	114.87	162.61	-21.14	-45.35	0.0 ^{b)}
1' (C ₂)	5.7629	112.04	158.05	-30.46	-49.03	6.3
2 (C ₁)	4.2725	105.57	7.52	-172.28	30.93	-34.8
			107.33	-77.65	-7.54	
MP2/Gen (the 6-311+G(3d) basis set for S and O with the 6-311G(d) basis set for C and H)						
I (A: C ₂)	5.7492	103.69	150.36	-33.84	-41.58	0.0 ^{c)}
I (D: C ₁)	4.5640	105.69	-8.47	172.87	41.41	24.8
			135.39	-50.54	-32.21	
1 (C ₂)	5.6964	113.51	167.78	-13.83	-54.95	0.0 ^{d)}
2 (C ₁)	4.4977	105.30	-4.39	176.77	37.82	24.4
			129.83	-54.92	-28.03	

a) $E = -1734.2873$ au. b) $E = -1963.3984$ au. c) $E = -1730.9682$ au. d) $E = -1959.5051$ au.

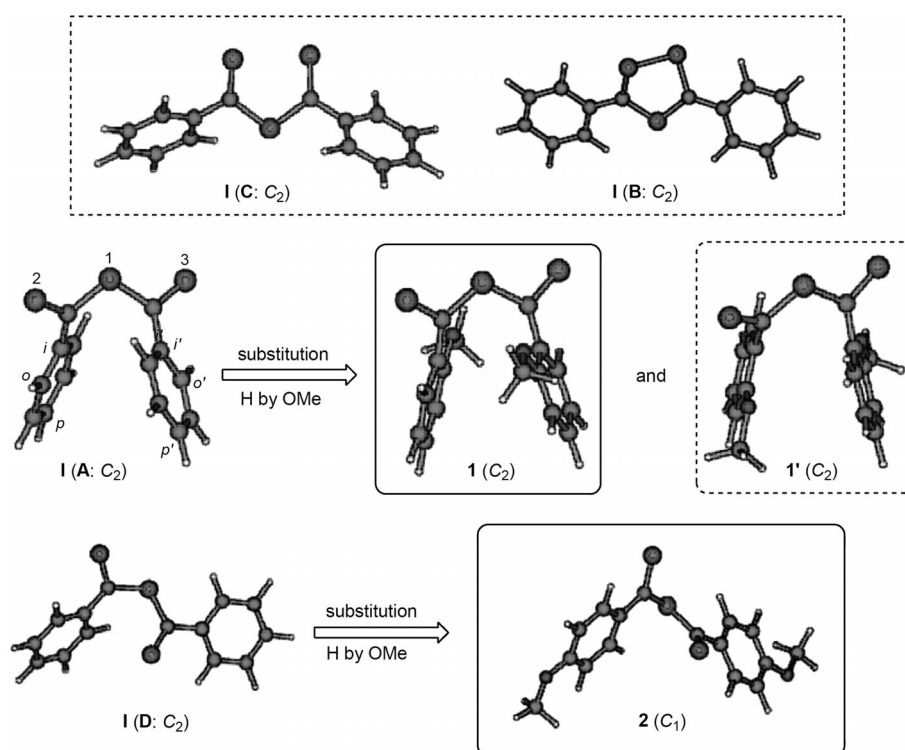


Figure 9. Formation of **1**, **1'**, and **2** through substitution of the hydrogen atoms of **I** by OMe groups. Compounds **1** and **2** are observed but not **1'** in the crystals.

The observed structure of **1** apparently forms through the substitution of hydrogen atoms at the o,o'-positions of **I** (A) by the methoxy groups. Only a slight change was observed in the structure of **1** in the optimization process with the methoxy groups, relative to the case of **I** (A). Another topological conformer of **1** (**1'**) could also exist as a stable conformer, where methoxy groups were introduced in place of the hydrogen atoms at the other o,o'-positions in **I** (A). A slight change was also detected in the optimization process for **1'**. **1'** is predicted to be less stable than **1** by 6.3 kJ·mol⁻¹, relative to **1**. Similarly,

a small change was observed in the optimization process of **2** with the methoxy groups, which was predicted to be more stable than **1**. The results are supported by the calculations at the MP2 level employing the 6-311+G(3d) basis set for sulfur and oxygen with the 6-311G(d) basis set for carbon and hydrogen. On the other hand, the observed structure of **2** forms through the substitution of the hydrogen atoms at the p,p'-positions in **I** (D) by the methoxy groups. A small change was observed in the structure of **2** in the optimization process with the methoxy groups. Compound **2** is predicted to be less stable

than **1**. Weak interactions such as π - π interactions are not well evaluated at the B3LYP level but they would be overestimated at the MP2 level, which must be responsible for the results of calculations at the two levels. Why **1** is observed, while the relative energy of **1'** is almost the same that of **1**? The structure in crystals must be stabilized or destabilized by the crystal packing effect. The effective volume of **1** is expected to be smaller than that of **1'**, since **1'** seems more extended form relative to **1**. The more densely packed crystals of **1**, due to its less effective volume, would also be advantageous to be observed in crystals.

UV/Vis Spectroscopy

The bis(arenecarbothioyl) sulfides and aromatic acyl thioacyl sulfides show quite characteristic colors of deep blue to green. In general, the $n \rightarrow \pi^*$ transitions of dithio esters appear in the range of 510–580 nm for aromatic dithioesters (RCSSR', R = aryl) with a small extinction coefficient due to the forbidden transition.^[13] Table 6 shows the electron spectra of compounds **1**, **2**, and **3b** along with their calculated values.

Table 6. Electron spectra of compounds **1**, **2**, and **3b**.

Compounds	λ max (oscillator strength) ^{a)}	λ max (log ϵ) ^{b)}	Ref.
	calculated values	experimental values	
(2-MeOC ₆ H ₄ CS) ₂ S (1)	399 (0.474)	385 (4.00)	3c
	511 (0.591)	531 (2.34)	
	627 (0.160)	580sh 614 (1.21)	
(4-MeOC ₆ H ₄ CS) ₂ S (2)	374 (0.540)	370 (4.56)	3b
	555 (0.242)	558 (2.36)	
	584 (0.619)	625sh	
2-MeOC ₆ H ₄ CO ₂ S 2-MeOC ₆ H ₄ CS ⁻ S (3b)	343 (0.554)	340 (4.03)	this work
	397 (0.643)	552 (2.30)	
	523 (0.149)	588sh ?	

a) Gas-phase vertical excitation energies are calculated with the with the 6-311+G(d) basis sets for S, O, C, and H at TD-DFT (B3LYP) level applied on the optimized structures at the MP2 level. b) In CH₂Cl₂.

As shown in Table 6, the electron spectra of compounds **1** (ap/ap-conformer) and **2** (sp/ac-conformer) had absorption maxima at ca. 600 nm and 620 nm, respectively, which are assignable to $n \rightarrow \pi^*$ transitions on the thiocarbonyl sulfur atom based on the magnitude of the extinction coefficient. Such bathochromic shifts of the $n \rightarrow \pi^*$ transitions of **1** and **2** may be explained in terms of the orbital interactions of the lone-pair electrons on the central sulfur atom with *anti*-bonding orbital $n \rightarrow \pi^*$ transitions (see Table 4: $n_{S(11)} \rightarrow \pi^*_{S(12)=C(11)}$, $n_{S(11)} \rightarrow \pi^*_{S(21)=C(11)}$). On the other hand, the corresponding $n \rightarrow \pi^*$ transitions of compound **3b** (sc/ap-conformer) appeared at 552 nm. Such a hypsochromic shift for **3b** may also be explained in terms of the orbital interactions of the lone-pair electrons on the central sulfur atom with the *anti*-bonding orbital $n \rightarrow \pi^*$ transitions (see Table 4: $n_{S(11)} \rightarrow \pi^*_{S(21)=C(21)}$ and $n_{S(21)} \rightarrow \sigma^*_{S(11)-C(21)}$).

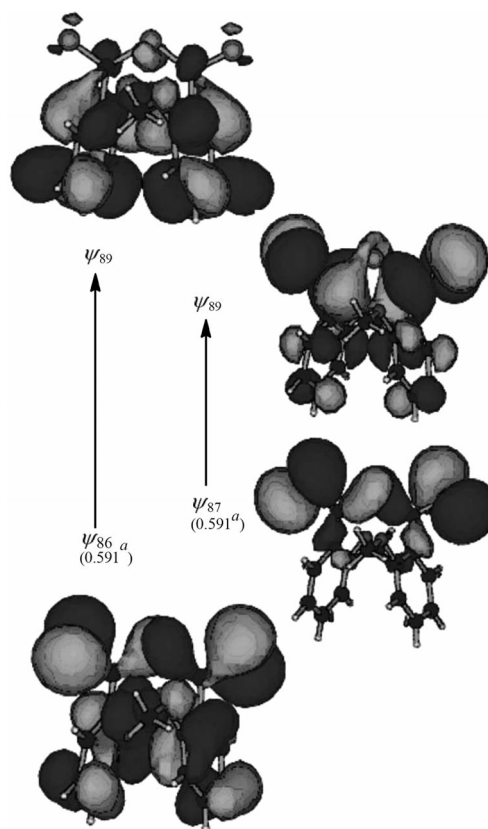


Figure 10. Molecular orbital presentation of the excited state 1 ($f = 0.017$) for *syn*-(2-MeOC₆H₄CS)₂S (**1**) ($\psi_{87} = \text{HOMO}$); the coefficient for the wavefunctions of each transition given by a .

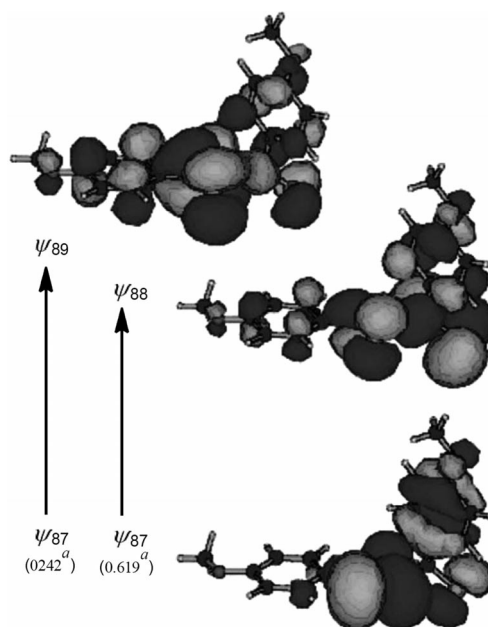


Figure 11. Molecular orbital presentation of the excited state 2 ($f = 0.003$) for *syn*-(4-MeOC₆H₄CS)₂S (**2**) ($\psi_{87} = \text{HOMO}$); the coefficient for the wavefunctions of each transition given by a .

Figure 10, Figure 11, and Figure 12 show the molecular orbital diagrams of excited state 1 ($f = 0.017$) for (2-MeOC₆-

$\text{H}_4\text{CS}_2\text{S}$ (**1**; ap/ap) (ψ_{87} = HOMO), excited state 2 ($f = 0.003$) for $(4\text{-MeOC}_6\text{H}_4\text{CS})_2\text{S}$ (**2**; ac/sp) (ψ_{87} = HOMO) and excited state 1 ($f = 0.003$) for $(2\text{-MeOC}_6\text{H}_4\text{CO})(2\text{-MeOC}_6\text{H}_4\text{CS})\text{S}$ (**3b**; sp/ap) (ψ_{83} = HOMO), respectively, where the $\psi_{86} \rightarrow \psi_{89}$, $\psi_{87} \rightarrow \psi_{89}$ and $\psi_{83} \rightarrow \psi_{85}$ transitions correspond to the symmetric-to-symmetric transitions of the *s*- and *p*-types are added, respectively.

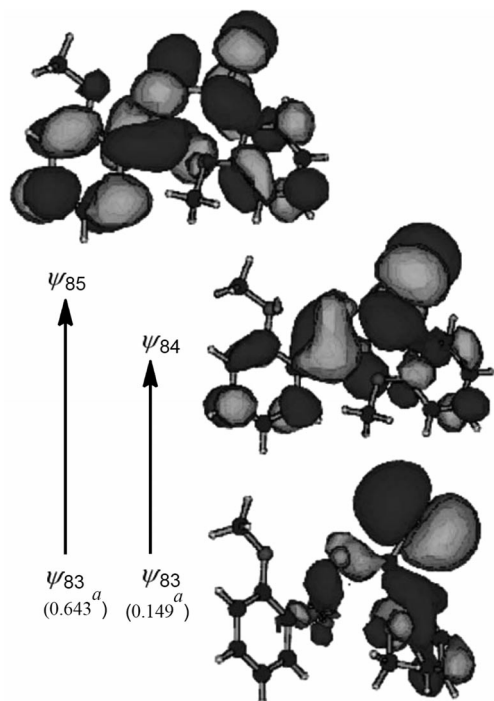


Figure 12. Molecular orbital presentation of the excited state 1 ($f = 0.0028$) for *syn*-(2-MeOC₆H₄CO)(2-MeOC₆H₄CS)S (**3b**) (ψ_{83} = HOMO); the coefficient for the wavefunctions of each transition given by *a*.

Concluding Remarks

The crystal structures of a series of $(2\text{-MeOC}_6\text{H}_4\text{CS})_2\text{S}$ (**1**), $(4\text{-MeOC}_6\text{H}_4\text{CS})_2\text{S}$ (**2**) and $(2\text{-MeOC}_6\text{H}_4\text{CO})(2\text{-MeOC}_6\text{H}_4\text{CS})\text{S}$ (**3b**) were compared with those of the corresponding oxygen derivatives $(2\text{-MeOC}_6\text{H}_4\text{CO})_2\text{S}$ (**4**), $(2\text{-MeOC}_6\text{H}_4\text{CO})_2\text{O}$ (**5**), $(4\text{-MeOC}_6\text{H}_4\text{CO})_2\text{O}$ (**6**). Compound **1** was an unusual saddle structure in which the $-\text{C}(=\text{S})-\text{S}-\text{C}(=\text{S})-$ moiety is planar and two benzene rings lie a face-to-face and in addition, no orbital interactions between the both atoms between the central sulfur atom and the 2-methoxy oxygen atoms, in spite of substantially short (3.07 Å). Such unusual structure of **1** was considered to be stabilized by the crystal packing effect, due to its less effective volume, rather than intramolecular interaction.

The deep blue to green colors of compounds **1** and **2** and the deep violet color of compound **3b** reflect the transitions of the lone-pair electrons in the HOMO (ψ_{87}) of the thiocarbonyl sulfur atom to the LUMO (ψ_{89}) and of the lone-pair electrons in the ψ_{83} (HOMO) of the thiocarbonyl sulfur atom to the LUMO (ψ_{85}).

These results may help us to understand the physical properties of other unstable sulfur, selenium and tellurium isologues of acid anhydride $[\text{RC}(=\text{E}^1)\text{E}^2\text{C}(=\text{E}^3)\text{R}']$, ($\text{E}^1, \text{E}^2, \text{E}^3 = \text{O}, \text{S}, \text{Se}, \text{Te}$; $\text{R}, \text{R}' = \text{alkyl}, \text{aryl}$), which could not be synthesized so far.

Experimental Section

The melting points were measured by a Yanagimoto micromelting point apparatus and uncorrected. The IR spectra were measured with a PERKIN ELMER FT-IR 1640 and a JASCO grating IR spectrophotometer IR-G. The ¹H-NMR and ¹³C-NMR spectra were recorded with JNM-α400 instruments at 399.7 and 100.4 MHz, respectively with tetramethylsilane as an internal standard. Electron spectra were measured with a JASCO U-Best 55. Mass spectra were recorded with a Shimadzu GC-MS QP1000 (A) (EI/CI, model) mass spectrometer. The high resolution mass spectroscopy (H.R. MS) was taken with a Shimadzu GC-MS 9020DF high resolution mass spectrometer. Elemental analyses were performed by the Elemental Analysis Center of Kyoto University.

Materials

4-Chlorobenzoyl, 4-methylbenzoyl, 2-methoxybenzoyl and 4-methoxybenzoyl chlorides were prepared according to the literature.^[14] Potassium arenecarbothioates were prepared by the reaction of the corresponding carbodithioic acids with potassium hydrides as described in the literature.^[15] Bis(2-methoxybenzoyl) sulfide and bis(2-methoxybenzoyl) anhydride were synthesized according to the literature.^[16,17]

X-ray Diffraction

The measurement was carried out with a Rigaku AFC7R four-circle diffractometer with graphite-monochromated Mo-*K*_α radiation ($\lambda = 0.71069$ Å). All of the structures were solved and refined using the teXsan crystallographic software package on an IRIS Indigo computer.^[18] X-ray quality crystals of **1**, **2**, and **3b** were obtained by recrystallization from ether/petroleum ether. These crystals were cut and coated with an epoxy resin and mounted on a glass fiber. The cell dimensions were determined from a least-squares refinement of the setting diffractometer angles for 25 automatically centered reflections. Lorentz and polarization corrections were applied to the data, and empirical absorption corrections (ψ -scans^[19]) were also applied. The structures were solved by direct method using SHELX-97^[20] and expanded using DIRDIF92.^[21] Scattering factors for neutral atoms were adapted according to Cromer and Waber^[22] and anomalous dispersion^[23] was used. The function minimized was $\sum w(|F_o| - |F_c|)^2$, and the weighting Scheme employed was $w = [\sigma^2(F_o) + p^2(F_o)^2/4]^{-1}$. A full-matrix least-squares refinement was executed with non-hydrogen atoms being anisotropic. The final least-square cycle included fixed hydrogen atoms at calculated positions of which each isotropic thermal parameter was set to 1.2 times of that of the connecting atom.

Bis(2-methoxybenzenecarbothioyl) sulfide (1): Yield: 77%. Mp (dec.): 102–104 °C. IR (KBr): 1245 (C=S), 1281 (C=S) cm⁻¹. ¹H NMR (400 MHz, CDCl₃): $\delta = 3.72$ (s, 6 H, CH₃O), 6.54 (d, $J = 7.8$ Hz, 2 H, arom), 6.76 (t, $J = 7.8$ Hz, 2 H, arom), 7.20 (t, $J = 7.8$ Hz, 2 H, arom) 7.28 (d, $J = 7.8$ Hz, 2 H, arom). ¹³C NMR (100 MHz, CDCl₃): $\delta = 55.5$ (CH₃O), 110.7, 120.4, 130.3, 132.8, 135.8, 154.1 (arom), 229.0 (C = S). The IR spectrum was in good agreement with that of

the authentic sample which was prepared from the condensation reaction of the corresponding carbodithioic acid with dicyclohexylcarbodiimide.^[3c]

Bis(4-methoxybenzenecarbothioyl) sulfide (2): Yield: 68%. Mp (dec.): 65–66 °C (65–66 °C^[3c]). IR (KBr): 1250, 1265 (C=S) cm⁻¹. ¹H NMR (400 MHz, CDCl₃): δ = 3.85 (s, 6 H, CH₃O), 6.83 (d, *J* = 9.0 Hz, 4 H, arom), 8.05 (t, *J* = 9.0 Hz, 4 H, arom). ¹³C NMR (100 MHz, CDCl₃): δ = 55.6 (CH₃O), 113.8, 130.3, 138.7, 164.5 (arom), 221.3 (C = S).

The spectroscopic data and physical properties were in good agreement with that of the authentic sample which was prepared from the condensation reaction of the corresponding carbodithioic acid with dicyclohexylcarbodiimide.^[3b]

Acyl Thioacyl Sulfides

For acyl thioacyl sulfides (**3**), the preparation procedures of (2-methoxybenzoyl)(2-methoxybenzenecarbothioyl) sulfide (**3b**) are described in detail. The spectroscopic data of the other compounds **3a** and **3c** are shown in the supporting information (Table S2).

(2-Methoxybenzoyl)(2-methoxybenzenecarbothioyl) sulfide (3b): A solution of 2-methoxybenzoyl chloride (0.144 g, 0.842 mmol) in dichloromethane (4 mL) was added to a suspension of potassium 2-methylbenzenecarbodithioate (0.197 g, 0.886 mmol) in the same solvent (20 mL) at 0 °C under argon atmosphere. The color of the solution gradually changed from red to reddish purple. The mixture was stirred at the same temperature for 2 h. The white precipitates (KCl) were filtered off. Removal of the solvent from the filtrate under reduced pressure (21 °C/3 Torr) gave a dark blue solid. Recrystallization from Et₂O (0.5 mL)/hexane (15 mL) yielded **3b** as dark blue crystals.

Yield: 0.217 g (81%). Mp (dec.): 94–100 °C. IR (KBr): 1677 (C=O), 1250 (C=S) cm⁻¹. ¹H NMR (400 MHz, CDCl₃): δ = 3.74 (s, 3 H, CH₃O), 3.90 (s, 3 H, CH₃O), 6.83 (d, *J* = 7.8 Hz, 1 H, arom-CS), 6.97 (d, *J* = 7.8 Hz, 1 H, arom-CO), 6.99 (t, *J* = 7.8 Hz, 1 H, arom-CO), 7.00 (t, *J* = 7.8 Hz, 1 H, arom-CO), 7.42 (t, *J* = 7.8 Hz, 1 H, arom-CS), 7.50 (d, *J* = 7.8 Hz, 1 H, arom-CS), 7.60 (t, *J* = 7.8 Hz, 1 H, arom-CO), 7.74 (d, *J* = 7.8 Hz, 1 H, arom-CO). ¹³C NMR (100 MHz, CDCl₃): δ = 55.7 (CH₃O), 55.8 (CH₃O), 110.7, 112.0, 120.6, 120.7, 125.2, 130.3, 130.4, 132.6, 134.7, 137.6, 154.0, 158.4 (arom), 185.4 (C=O), 229.5 (C = S). UV/Vis: λ_{max} (lg ε) (CH₂Cl₂): 222 nm (4.53), 269 (4.00), 340 (4.03), 552 (2.34). C₁₆H₁₄O₃S₂ (318.40): found C 59.90 (calc 60.35), H 4.55 (4.43)%.

Bis(2-Methoxybenzoyl) sulfide (4): Yield: 0.165 g (62%). Mp (dec.): 66–69 °C (Ref. [16] 65–67 °C).

IR (KBr): 1732 (C=O), 1662 (C=O) cm⁻¹. ¹H NMR (400 MHz, CDCl₃): δ = 3.87 (s, 6 H, CH₃O), 6.96 (d, *J* = 7.9 Hz, 2 H, arom), 7.00 (t, *J* = 7.9 Hz, 2 H, arom), 7.48 (t, *J* = 7.71 (d, 7.9 Hz, 2 H, arom). ¹³C NMR (100 MHz, CDCl₃): δ = 55.8 (CH₃O), 112.0, 120.4, 127.4, 130.2, 134.2, 157.8 (arom), 186.4 (C=O).

2-Methoxybenzoic anhydride (5):^[17] Yield: 0.165 g (62%). Mp (dec.): 70–73 °C. IR (KBr): 1733 (C=O) cm⁻¹. ¹H NMR (400 MHz, CDCl₃): δ = 3.85 (s, 6 H, CH₃O), 7.00 (d, *J* = 8.0 Hz, 2 H, arom), 7.03 (t, *J* = 8.0 Hz, 2 H, arom), 7.55 (t, *J* = 8.0 Hz, 2 H, arom), 8.01 (t, *J* = 8.0 Hz, 2 H, arom). ¹³C NMR (100 Hz, CDCl₃): δ = 55.9 (CH₃O), 112.1, 118.1, 120.3, 133.0, 135.2, 160.1 (arom), 161.9 (C=O).

Supporting Information (see footnote on the first page of this article): Experimental part, Figure S1, Table S1, and Table S2.

Acknowledgments

This research was by a Grant-in-Aid for Scientific Research on Priority Areas and by a Grant-in-Aid for Scientific Research from the Ministry of Education, Science, Sports and Culture of Japan. We thank *Emeritus Prof. Takashi Kawamura* of Gifu University for invaluable advices with X-ray crystallography. We also thank *Prof. Mao Minoura* for valuable advices with the depictions of the molecular structures.

References

- O. Niyomura, R. Yamada, S. Nakaiida, M. Ishida, M. Ebihara, S. Kato, F. Ando, J. Koketsu, *Molecules*, **2009**, *14*, 2555–2572; doi: 10.3390.
- a) S. Kato, K. Sugino, M. Yamada, T. Kanda, M. Mizuta, *Angew. Chem. Int. Ed. Engl.* **1977**, *16*, 879–880; b) S. Kato, K. Sugino, Y. Matsuzawa, T. Katada, I. Noda, M. Mizuta, M. Goto, M. Mizuta, *Liebigs Ann. Chem.* **1981**, 1798–1811; c) S. Kato, H. Masumoto, S. Ikeda, M. Itoh, T. Murai, H. Ishida, *Z. Chem.* **1990**, *30*, 67–69.
- a) S. Kato, T. Katada, M. Mizuta, *Angew. Chem. Int. Ed. Engl.* **1976**, *15*, 766–880; b) S. Kato, H. Shibahashi, T. Katada, T. Takagi, I. Noda, M. Mizuta, M. Goto, M. Mizuta, *Liebigs Ann. Chem.* **1982**, 1229–1244; c) S. Kato, H. Masumoto, M. Kimura, T. Murai, M. Ishida, *Synthesis* **1987**, 304–307.
- For cyclic derivatives: a) M. V. Lakshmikantham, P. Carroll, G. Furst, M. I. Levinson, M. P. Cava, *J. Am. Chem. Soc.* **1984**, *106*, 6084–6085; b) M. S. Raasch, N. Z. Huang, M. V. Lakshmikantham, M. P. Cava, *J. Org. Chem. Soc.* **1988**, *53*, 891–893; c) M. V. Lakshmikantham, W. Chen, M. P. Cava, *J. Org. Chem. Soc.* **1989**, *54*, 4746–4750.
- S. Yoneda, K. Okazaki, K. Yanagi, M. Minobe, *J. Chem. Soc., Chem. Commun.* **1986**, 19–20.
- F. Iwasaki, M. Sakuratani, M. Yasui, N. Kamiya, H. Iwasaki, *Bull. Univ. Electro-Commun.* **1995**, *8*, 89–94; F. Iwasaki, M. Sakuratani, H. Kaneko, M. Yasui, N. Kamiya, H. Iwasaki, *Acta Crystallogr., Sect. B* **1995**, *51*, 1028–1035.
- CCDC Data Base search for aromatic acid anhydrides (ArCO)₂O resulted in 6 hits: (2-MeOC₆H₄CO)₂O (refcode: ASPRIN); (4-BrC₆H₄CO)₂O (refcode: BBENAN and BBENAN01); (4-ClC₆H₄CO)₂O (refcode: CLBNAH); (4-NO₂C₆H₄CO)₂O (refcode: VIFBAN); (4-Me₂NC₆H₄CO)₂O (refcode: YENKEH); (9-anthroyl)₂O (refcode: YUYEK). The interplaner-angle O¹=C¹–C²=O² of these compounds are in the range of 17.5–77.4°.
- IUPAC, *Compendium of Chemical Terminology*, 2nd ed. Blackwell Scientific Publication, Oxford, UK, **1997**; Basic Terminology of Stereochemistry (IUPAC Recommendations, **1996**), p. 2199.
- M. Nishio, *The CH/π Interaction. Evidence, Nature and Consequences*, Wiley-VCH, New York, **1998**; M. Nishio, *Cryst-EngComm* **2004**, *6*, 138–158; O. Takahashi, Y. Kohno, M. Nishio, *Chem. Rev.* **2010**, *110*, 6049–6076.
- A. D. Becke, *Phys. Rev. Sect. A* **1988**, *38*, 3100; A. D. Becke, *J. Chem. Phys.* **1993**, *98*, 5648–5652.
- C. Lee, W. Yang, R. G. Parr, *Phys. Rev. Sect. B* **1988**, *37*, 785–789; B. Miehlich, A. Savin, H. Stroll, H. Preuss, *Chem. Phys. Lett.* **1989**, *157*, 200–206.
- Gaussian 2003, 2004*, M. J. Frisch, G. W. Trucks, H. B. Schlegel, G. E. Scuseria, M. A. Robb, J. R. Cheeseman, J. A. Montgomery Jr., T. Vreven, K. N. Kudin, J. C. Burant, J. M. Millam, S. S. Iyengar, J. Tomasi, V. Barone, B. Mennucci, M. Cossi, G. Scalmani, N. Rega, G. A. Petersson, H. Nakatsuji, M. Hada, M. Ehara, K. Toyota, R. Fukuda, J. Hasegawa, M. Ishida, T. Nakajima, Y.

- Honda, O. Kitao, H. Nakai, M. Klene, X. Li, J. E. Knox, H. P. Hratchian, J. B. Cross, C. Adamo, J. Jaramillo, R. Gomperts, R. E. Stratmann, O. Yazyev, A. J. Austin, R. Cammi, C. Pomelli, J. W. Ochterski, P. Y. Ayala, K. Morokuma, G. A. Voth, P. Salvador, J. J. Dannenberg, V. G. Zakrzewski, S. Dapprich, A. D. Daniels, M. C. Strain, O. Farkas, D. K. Malick, A. D. Rabuck, K. Raghavachari, J. B. Foresman, J. V. Ortiz, Q. Cui, A. G. Baboul, S. Clifford, J. Cioslowski, B. B. Stefanov, G. Liu, A. Liashenko, P. Piskorz, I. Komaromi, R. L. Martin, D. J. Fox, T. Keith, M. A. Al-Laham, C. Y. Peng, A. Nanayakkara, M. Challacombe, P. M. W. Gill, B. Johnson, W. Chen, M. W. Wong, C. Gonzalez, J. A. Pople, Gaussian, Inc., Pittsburgh PA, **2003**.
- [13] S. Scheithauer, R. Mayer, *Topics in Sulfur Chemistry*, Vol. 4, George Thieme Publishers, Stuttgart, **1979**, p. 181–191.
- [14] R. B. Wagner, H. D. I. Zook, in: *Synthetic Organic Chemistry*, John Wiley & Sons: New York, **1965**, p. 546.
- [15] S. Kato, S. Yamada, H. Goto, K. Terashima, M. Mizuta, T. Katada, *Z. Naturforsch.* **1980**, 35b, 458–462; S. Kato, N. Kitaoka, O. Niyomura, Y. Kito, T. Kanda, M. Ebihara, *Inorg. Chem.* **1999**, 38, 519–530.
- [16] H. Masumoto, T. Tsutsumi, T. Kanda, M. Komada, T. Murai, S. Kato, *Sulfur Lett.* **1989**, 10, 103–115.
- [17] P. Rambacher, S. Make, *Angew. Chem.* **1968**, 80, 487.
- [18] *teXsan*: Crystal Structure Analysis Package, Molecular Structure Corporation (**1985, 1992**).
- [19] A. C. T. North, D. C. Phillips, F. S. Mathews, *Acta Crystallogr., Sect. A* **1968**, 24, 351–359.
- [20] G. M. Sheldrick, *SHELXL97*, Program for the Refinement of Crystal Structure, University of Göttingen, Germany, **1997**.
- [21] The *DIRDIF program system*: P. T. Beuvskens, G. Admiraal, G. Beurskens, W. P. Bosman, S. Garcia-Granda, R. O. Gould, J. M. M. Smits, C. Smykalla, *Technical Report of the Crystallography Laboratory*; University of Nijmegen: The Netherlands, **1992**.
- [22] D. T. Cromer, J. T. Waber, *International Tables for X-ray Crystallography*, The Kynoch Press: Birmingham, U. K., **1974**; Vol. 4, Table 2.2A.
- [23] D. C. Creagh, W. J. McAuley, *International Tables for X-ray Crystallography* (Ed.: A. J. C. Wilson), Kluwer Academic Publ. Boston, **1992**; Vol. C, Table 4.2.6.8, pp. 219–222.

Received: August 1, 2012

Published Online: December 3, 2012